7

A New Waveform based on Linear Precoded Multicarrier Modulation for Future Digital Video Broadcasting Systems

Oudomsack Pierre Pasquero, Matthieu Crussière, Youssef Nasser, Eddy Cholet and Jean-François Hélard
European University of Brittany (UEB)
Institute of Electronics and Telecommunications of Rennes (IETR)
INSA de Rennes, 20, avenue des Buttes de Coesmes, 35043 Rennes, France

1. Introduction

Orthogonal Frequency Division Multiplexing (OFDM) has been perceived as one of the most effective transmission schemes for multipath propagation channels. It has been widely adopted in most of the digital video broadcasting (DVB) standards such as DVB-T in Europe, DMB-T in China, FLO in North America, ISDB-T in Japan. The major reason for this success lies in the capability of OFDM to split the single channel into multiple parallel intersymbol interference (ISI) free subchannels. It is easily carried out by implementing Inverse Fast Fourier Transform (IFFT) at the transmitter and Fast Fourier Transform (FFT) at the receiver [1]. Therefore, the distortion associated to each subchannel, also called subcarrier, can be easily compensated for by one coefficient equalization. For that purpose, the receiver needs to estimate the channel frequency response (CFR) for each subcarrier. In the DVB-T standard [2], one subcarrier over twelve is used as pilot for CFR estimation as illustrated in Fig. 1, i.e. symbols known by the receiver are transmitted on these subcarriers. Thus, the receiver is able to estimate the CFR on these pilot subcarriers and to obtain the CFR for any subcarrier using interpolating filtering techniques [3].
Nevertheless, OFDM systems are very sensitive to synchronization error such as carrier frequency offset (CFO) or sampling frequency offset (SFO) [4]. Indeed, when the carrier frequency or the sampling frequency of the transmitter and the receiver are not equal, the orthogonality between the different subcarriers is lost which can lead to strong intercarrier interference (ICI) effects [4]. This is why in addition to the scattered pilot subcarriers used for CFR estimation, continuous pilot subcarriers have been defined in the DVB-T standard [2] to estimate the CFO and the SFO [5]. Fig. 1 depicts the locations of the data subcarriers and the pilot subcarriers over the time and frequency grid as defined in the DVB-T standard. The originality of this work is to reduce the overhead part resulting from pilot insertion by using a joint CFR, CFO and SFO estimation approach based on a linear precoding function. Eventually, these pilots dramatically reduce the spectral efficiency and the useful bit rate of the system. The basic idea consists in using a two-dimensional (2D) linear

Source: Digital Video, Book edited by: Floriano De Rango,
ISBN 978-953-7619-70-1, pp. 500, February 2010, INTECH, Croatia, downloaded from SCIYO.COM

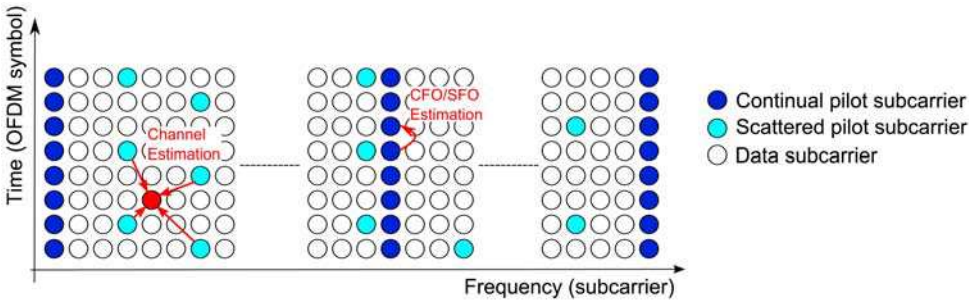

Fig. 1. Data and Pilot subcarriers locations over the time and frequency grid in the DVB-T standard

precoding matrix before the OFDM modulation, and to dedicate one of the precoding sequences to transmit a so-called *spread pilot* information [6]. It will be showed that these spread pilots can provide a diversity gain for some estimators. Moreover, the 2D linear precoding function improves the flexibility of the system compared to the DVB-T standard.
This chapter is organized as follows. In section 2, we describe the proposed transmitter scheme based on spread pilots. The transmitted signal and the pilot symbols insertion technique are studied. In section 3, the proposed channel estimation principle based on spread pilot is described in perfect synchronization case. The analytical expression of the mean square error (MSE) of the estimator is derived. Some simulation results in term of bit error rate (BER) of the proposed CFR estimation are given and compared with those of the DVB-T standard. The proposed synchronization algorithms are presented in section 4. Two different stages of CFO and SFO estimations are considered. The first one is dedicated to the fine synchronization. The second one is used to estimate the residual CFO and SFO. Some simulation results in term of BER and mean square error (MSE) of the estimators are given and analized. Finally, we conclude this chapter by a general comparison between the proposed system based on spread pilots and the DVB-T standard in term of performance, complexity and flexibility.

2. Transmitter scheme

The transmitter structure on which spread pilot principles are based is depicted in Fig. 2. We consider an OFDM communication system using N subcarriers, N_u of which being active, with a guard interval size of υ samples. In the first step, data bits are encoded, interleaved and converted to complex symbols $x_{t,s}[i]$, assumed to have zero mean and unit variance. These data symbols are then interleaved before being linearly precoded (LP) by a sequence $\mathbf{c}_i$ of L chips, with $0 \le i \le L = 2^n$ and $n \in \mathbb{N}$. The sequences used for the precoding function are the well-known Walsh-Hadamard (WH) codes [7] [8]. They have been choosen for their orthogonality property. The chips obtained are mapped over a subset of $L = L_t \times L_f$ subcarriers, with L_t and L_f defined as the time and frequency spreading factors respectively. The first L_t chips are allocated in the time direction. The next blocks of L_t chips are allocated identically on the adjacent subcarriers as illustrated in Fig. 3. Therefore, the 2D chip mapping follows a zigzag in time. Let us note that the way of applying the 2D chip mapping does not change significantly the system performance [9].

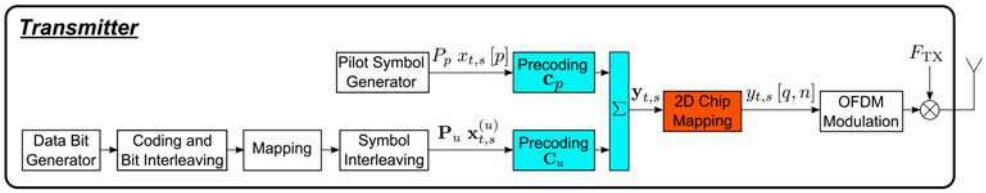

Fig. 2. 2D LP OFDM transmitter based on spread pilots

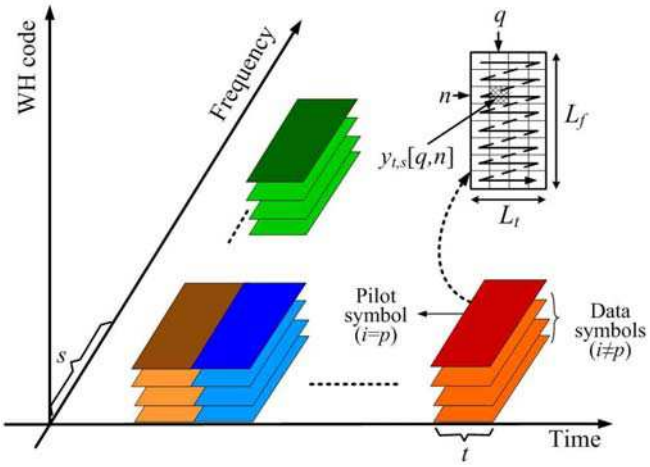

Fig. 3. 2D Spreading Scheme

Inspired by pilot embedded techniques [10], spreading the pilot symbols consists in transmitting low level pilot-sequences concurrently with the data. In order to reduce the cross-interferences between pilots and data, the idea is to select a pilot sequence which is orthogonal with the data sequences. This is obtained by allocating one of the WH orthogonal sequences $\mathbf{c}_p$ to the pilots symbols $x_{t,s}[p]$ on every subset of subcarriers. Contrary to the DVB-T system where the pilot symbols are transmitted by only a few subcarriers, in the proposed system each active subcarrier conveys a part of the spread pilot information. Consequently, numerous observation samples are avaible and the estimators can benefit from the frequency diversity of the channel over the whole bandwidth. Nevertheless, since each pilot symbol is superimposed to $(L-1)$ data symbols, as illustrated in Fig. 3, a term of interference appears if the orthogonality is lost.

To derive the appropriate estimation algorithms in the sequel, we need to formalize the transmitted signal expression. Therefore, we define a frame as a set of L_t adjacent OFDM symbols, and a sub-band as a set of L_f adjacent subcarriers. In order to distinguish between the different subsets of subcarriers, let us denote t and s the indexes referring to the frame and the sub-band respectively, with $0 \leq s \leq S-1$. Given these notations, we can express the signal transmitted on a subset of subcarriers (t, s):

$$\mathbf{y}_{t,s} = \mathbf{C}\,\mathbf{P}\,\mathbf{x}_{t,s} \tag{1}$$

where $\mathbf{x}_{t,s} = [x_{t,s}[0] \ldots x_{t,s}[i] \ldots x_{t,s}[L-1]]^T$ is the complex symbol vector, $\mathbf{P} = \text{diag}\left\{\sqrt{P_0} \ldots \sqrt{P_i} \ldots \sqrt{P_{L-1}}\right\}$ is a diagonal matrix which elements are amplitude weighting factors associated to symbols, and $\mathbf{C} = [\mathbf{c}_0 \ldots \mathbf{c}_i \ldots \mathbf{c}_{L-1}]$ is the WH precoding matrix which ith column corresponds to ith precoding sequence $\mathbf{c}_i = [c_i[0, 0] \ldots c_i[q, n] \ldots c_i[L_t - 1, L_f - 1]]^T$. We assume normalized precoding sequences, i.e. $c_i[q,n] = \pm\frac{1}{\sqrt{L}}$. Note that power factor P_p can advantageously be used as a boost factor for pilot symbols in order to help CFR estimation and synchronization procedures. Since the applied 2D chip mapping follows a zigzag in time, $c_i[q, n]$ is the $(n \times L_t + q)$th chip of the ith precoding sequence $\mathbf{c}_i$. Hence, the signal transmitted on the qth OFDM symbol and the nth subcarrier of the subset of subcarriers (t, s) writes:

$$y_{t,s}[q,n] = \sum_{i=0}^{L-1} \sqrt{P_i}\, x_{t,s}[i]\, c_i[n \times L_t + q] \tag{2}$$

3. Channel estimation

A. Principles

Let us define $\mathbf{H}_{t,s} = \text{diag}\{h_{t,s}[0, 0] \ldots h_{t,s}[q, n] \ldots h_{t,s}[L_t - 1, L_f - 1]\}$ as the $[L \times L]$ diagonal matrix of the channel frequency coefficients associated to a given subset of subcarriers (t, s). In perfect synchronization case and considering that the guard interval can absorb all the interference due to previous symbols, after OFDM demodulation and 2D chip de-mapping the received signal simply writes:

$$\mathbf{z}_{t,s} = \mathbf{H}_{t,s}\, \mathbf{y}_{t,s} + \mathbf{w}_{t,s} \tag{3}$$

where $\mathbf{w}_{t,s} = [w_{t,s}[0, 0] \ldots w_{t,s}[q, n] \ldots w_{t,s}[L_t - 1, L_f - 1]]^T$ is the additive white Gaussian noise (AWGN) vector having zero mean and variance $\sigma_w^2 = E\{|w_{t,s}[q, n]|^2\}$.

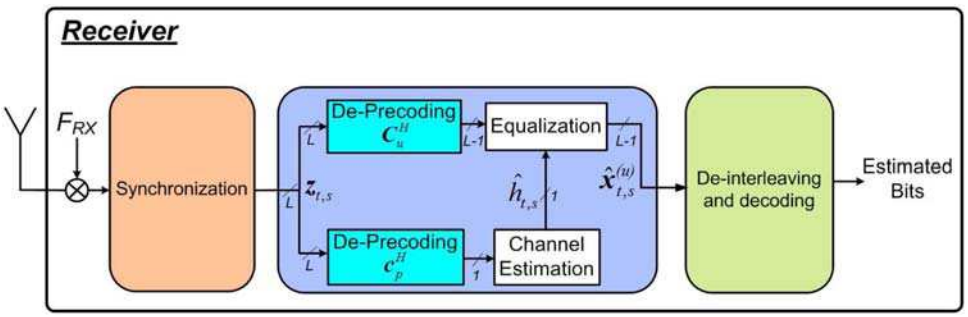

Fig. 4. Channel estimation scheme based on spread pilot

Fig. 4 depicts the receiver structure based on spread pilot CFR estimation. The basic idea of the proposed spread pilot CFR estimation algorithm is to estimate one average channel frequency coefficient $\hat{h}_{t,s}$ by subset of subcarriers (t, s). It is obtained by deprecoding the received signal $\mathbf{z}_{t,s}$ by the pilot sequence $\mathbf{c}_p^H$ and then dividing by the pilot symbol known by the receiver:

$$\begin{aligned}\widehat{h}_{t,s} &= \frac{1}{\sqrt{P_p}\, x_{t,s}\,[p]}\, \mathbf{c}_p^{\mathrm{H}}\, \mathbf{z}_{t,s} \\ &= \frac{1}{\sqrt{P_p}\, x_{t,s}\,[p]}\, \mathbf{c}_p^{\mathrm{H}}\, (\mathbf{H}_{t,s}\, \mathbf{C}\, \mathbf{P}\, \mathbf{x}_{t,s} + \mathbf{w}_{t,s})\end{aligned} \tag{4}$$

Let us denote $\mathbf{C}_u = [\mathbf{c}_0 \ldots \mathbf{c}_{i\neq p} \ldots \mathbf{c}_{L-1}]$ the $[L \times (L-1)]$ useful data precoding matrix, $\mathbf{P}_u = \mathrm{diag}\left\{\sqrt{P_0} \ldots \sqrt{P_{i\neq p}} \ldots \sqrt{P_{L-1}}\right\}$ the $[(L-1) \times (L-1)]$ diagonal matrix which entries are the amplitudes assigned to the data symbols, and $\mathbf{x}_{t,s}^{(u)} = [x_{t,s}[0] \ldots x_{t,s}\,[i \neq p] \ldots x_{t,s}\,[L-1]]^{\mathrm{T}}$ the $[(L-1) \times 1]$ data symbols vector. Given these notations, (4) can be rewritten as:

$$\begin{aligned}\widehat{h}_{t,s} &= \frac{1}{\sqrt{P_p}\, x_{t,s}\,[p]} \left(\mathbf{c}_p^{\mathrm{H}}\, \mathbf{H}_{t,s}\, \mathbf{c}_p\, \sqrt{P_p}\, x_{t,s}\,[p] + \mathbf{c}_p^{\mathrm{H}}\, \mathbf{H}_{t,s}\, \mathbf{C}_u\, \mathbf{P}_u\, \mathbf{x}_{t,s}^{(u)} + \mathbf{c}_p^{\mathrm{H}}\, \mathbf{w}_{t,s}\right) \\ &= \frac{1}{L}\mathrm{tr}\left\{\mathbf{H}_{t,s}\right\} + \frac{1}{\sqrt{P_p}\, x_{t,s}\,[p]} \left(\mathbf{c}_p^{\mathrm{H}}\, \mathbf{H}_{t,s}\, \mathbf{C}_u\, \mathbf{P}_u\, \mathbf{x}_{t,s}^{(u)}\right) + \frac{1}{\sqrt{P_p}\, x_{t,s}\,[p]} \left(\mathbf{c}_p^{\mathrm{H}}\, \mathbf{w}_{t,s}\right) \\ &= \overline{h}_{t,s} + \Xi_{\mathrm{MCI}}\,(t,s) + \Xi_{\mathrm{WGN}}\,(t,s)\end{aligned} \tag{5}$$

The first term $\overline{h}_{t,s}$ actually corresponds to the average CFR globally experienced by the subset of subcarriers (t, s). The second term represents the multiple code interference (MCI). It results from the loss of orthogonality between the precoding sequences caused by the variance of the channel frequency coefficients over the subset of subcarriers (t, s). One can actually check that if the channel coefficients are the same over the subset of subcarriers (t, s) which implies $\mathbf{H}_{t,s} = \overline{h}_{t,s}\mathbf{I}$, with $\mathbf{I}$ the $[L \times L]$ identity matrix, the MCI term is null because of the orthogonality between the sequences $\mathbf{c}_i$. The last term is the noise sample obtained after despreading. Finally, the estimated channel frequency coefficient (5) is used to equalize the $(L-1)$ data symbols spread over the same subset of subcarriers.

B. Estimator analysis

In order to analyze the theoretical performance of the proposed estimator, we propose to derive its MSE expression under the assumption of a wide-sense stationary uncorrelated scattering (WSSUS) channel [11].

$$\begin{aligned}\mathrm{MSE}\left\{\widehat{h}_{t,s}\right\} &= \mathrm{E}\left\{\left|\widehat{h}_{t,s} - \overline{h}_{t,s}\right|^2\right\} \\ &= \mathrm{E}\left\{\left|\Xi_{\mathrm{MCI}}\,(t,s)\right|^2\right\} + \mathrm{E}\left\{\left|\Xi_{\mathrm{WGN}}\,(t,s)\right|^2\right\}\end{aligned} \tag{6}$$

First, let us compute the MCI variance:

$$\mathrm{E}\left\{\left|\Xi_{\mathrm{MCI}}\,(t,s)\right|^2\right\} = \frac{1}{P_p}\mathrm{E}\left\{\mathbf{c}_p^{\mathrm{H}}\, \mathbf{H}_{t,s}\, \mathbf{C}_u\, \mathbf{P}'_u\, \mathbf{C}_u^{\mathrm{H}}\, \mathbf{H}_{t,s}^{\mathrm{H}}\, \mathbf{c}_p\right\} \tag{7}$$

where $\mathbf{P}'_u = \mathbf{P}_u\, \mathbf{P}_u^{\mathrm{H}} = \mathrm{diag}\left\{P_0 \ldots P_{i\neq p} \ldots P_{L-1}\right\}$. Actually, (7) cannot be analyzed practically due to its complexity. Applying some properties of random matrix and free probability theories [12] [13] which are stated in Appendix, a new MCI variance formula can be derived:

$$\begin{aligned}\mathrm{E}\left\{\left|\Xi_{\mathrm{MCI}}\left(t,s\right)\right|^2\right\} &= \frac{1}{P_p}\mathrm{E}\left\{\mathbf{c}_p^{\mathrm{H}}\,\mathbf{H}_{t,s}\left(\mathbf{I}-\mathbf{c}_p\,\mathbf{c}_p^{\mathrm{H}}\right)\mathbf{H}_{t,s}^{\mathrm{H}}\,\mathbf{c}_p\right\}\\ &= \frac{1}{P_p}\mathrm{E}\left\{\mathbf{c}_p^{\mathrm{H}}\,\mathbf{H}_{t,s}\,\mathbf{H}_{t,s}^{\mathrm{H}}\,\mathbf{c}_p-\mathbf{c}_p^{\mathrm{H}}\,\mathbf{H}_{t,s}\,\mathbf{c}_p\,\mathbf{c}_p^{\mathrm{H}}\,\mathbf{H}_{t,s}^{\mathrm{H}}\,\mathbf{c}_p\right\}\\ &= \frac{1}{P_p}\mathrm{E}\left\{\underbrace{\frac{1}{L}\mathrm{tr}\left\{\mathbf{H}_{t,s}\,\mathbf{H}_{t,s}^{\mathrm{H}}\right\}}_{A}-\frac{1}{L^2}\underbrace{\mathrm{tr}\left\{\mathbf{H}_{t,s}\right\}\mathrm{tr}\left\{\mathbf{H}_{t,s}^{\mathrm{H}}\right\}}_{B}\right\}\end{aligned} \tag{8}$$

The expectation of A is the average power of the channel frequency coefficients on the subset of subcarriers (t, s). Assuming that the channel frequency coefficients are normalized, its value is one:

$$\begin{aligned}\mathrm{E}\left\{\frac{1}{L}\mathrm{tr}\left(\mathbf{H}_{t,s}\,\mathbf{H}_{t,s}^{\mathrm{H}}\right)\right\} &= \frac{1}{L}\sum_{q=0}^{L_t-1}\sum_{n=0}^{L_f-1}\mathrm{E}\left\{\left|h_{t,s}\left[q,n\right]\right|^2\right\}\\ &= 1\end{aligned} \tag{9}$$

The expectation of B is a function of the autocorrelation of the channel R_{HH} (Δq,Δn) which expression (43) is developed in Appendix. Indeed, it can be written:

$$\mathrm{E}\left\{\left|\Xi_{\mathrm{MCI}}\right|^2\right\} = \frac{1}{P_p}\left(1-\frac{1}{L^2}\sum_{q=0}^{L_t-1}\sum_{n=0}^{L_f-1}\sum_{q'=0}^{L_t-1}\sum_{n'=0}^{L_f-1}R_{HH}\left(\Delta q,\Delta n\right)\right) \tag{10}$$

Now, let us compute the noise variance:

$$\begin{aligned}\mathrm{E}\left\{\left|\Xi_{\mathrm{WGN}}\right|^2\right\} &= \frac{1}{P_p}\mathrm{E}\left\{\mathbf{c}_p^{\mathrm{H}}\,\mathbf{w}_{t,s}\,\mathbf{w}_{t,s}^{\mathrm{H}}\,\mathbf{c}_p\right\}\\ &= \frac{1}{P_p}\frac{1}{L}\mathrm{E}\left\{tr\left\{\mathbf{w}_{t,s}\,\mathbf{w}_{t,s}^{\mathrm{H}}\right\}\right\}\\ &= \frac{1}{P_p}\sigma_w^2\end{aligned} \tag{11}$$

Finally, by combining the expressions of the MCI variance (10) and the noise variance (11), the MSE (6) writes:

$$\mathrm{MSE}\left\{\widehat{h}_{t,s}\right\} = \frac{1}{P_p}\left(1-\frac{1}{L^2}\sum_{q=0}^{L_t-1}\sum_{n=0}^{L_f-1}\sum_{q'=0}^{L_t-1}\sum_{n'=0}^{L_f-1}R_{HH}\left(\Delta q,\Delta n\right)+\sigma_w^2\right) \tag{12}$$

The analytical expression of the MSE depends on the pilot power P_p, also called boost factor, the autocorrelation function of the channel R_{HH} (Δq,Δn) and the noise variance σ_w^2. The autocorrelation of the channel (43) is a function of both the coherence bandwidth and the coherence time. We can then expect that the proposed estimator will be all the more efficient than the channel coefficients will be highly correlated within each subset of subcarriers. One

can actually check that if the channel is flat over a subset of subcarriers, then the MCI (10) is null. Therefore, it is important to optimize the time and frequency spreading lengths L_t and L_f , according to the transmission scenario. It is clear from (12) that the greater the boost factor P_p, the better the CFR estimator performance. On the other hand, the greater the boost factor P_p, the lower the data symbol power and the harder the data symbol detection. Therefore, the boost factor P_p has to be optimized in term of BER.

C. Simulation results

In this section, we analyse the performance of the proposed 2D LP OFDM system based on spread pilot CFR estimation compared to the DVB-T system with perfect CFR estimation. Table I gives the simulation parameters. The time-invariant channel models used are the F1 and P1 models detailed in [2]. They are specified for fixed outdoor rooftop antenna reception. The F1 channel corresponds to a line-of-sight (LOS) transmission, contrary to the P1 channel model which corresponds to a non-LOS transmission. The COST207 Typical Urban 6 paths (TU6) channel model is used as mobile channel. We define parameter β as the relative Doppler frequency equal to the product between the maximum Doppler frequency and the total OFDM symbol duration T_{OFDM}.

Bandwidth	8 MHz
FFT size (N_{FFT})	2048 samples
Guard Interval size	512 samples (64 μs)
OFDM symbol duration (T_{OFDM})	280 μs
Carrier frequency	500 MHz
Data symbol constellations	QPSK - 16QAM - 64QAM
Pilot symbol constellation	BPSK
Convolutional code rate	$R_c = 1/2$ using $(133, 171)_o$
Time-invariant channel models	F1 and P1
Mobile channel model	TU6 - 20km/h
Relative Doppler frequency	β=0.003

Table I Simulation parameters

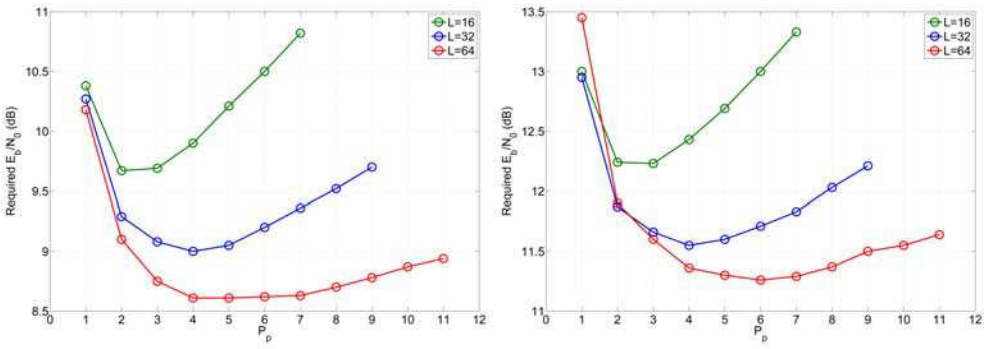

Fig. 5. Required $\frac{E_b}{N_0}$ to obtain a BER = 10^{-4} versus pilot power Pp - Spread Pilot Channel Estimation - 16QAM - Rc = 1/2

As it has been previously mentioned, it is important to optimize the boost factor Pp in function of the total spreading length L. For that purpose, Fig. 5(a) and Fig. 5(b) give the required $\frac{E_b}{N_0}$ (energy per bit to noise power spectral density ratio) to obtain a BER equal to 10^{-4} at the output of the Viterbi decoder for 16QAM data symbols under the F1 and the TU6 channel models respectively. It is noticeable that the boost factor values for which the required $\frac{E_b}{N_0}$ values reach a minimum, are similar for the time-invariant (F1) and the mobile (TU6) channels. Therefore, it is not necessary to adapt the boost factor in function of the channel characteristics. Moreover, for a given total spreading length, several values of Pp give similar performance in term of BER. Among these boost factor values, we will choose the largest one in order to obtain better estimators. In the following, the boost factor Pp will be equal to 3, 5 and 7 for a total spreading length of 16, 32 and 64 respectively.

The boost factor values optimized, we can analyze the CFR estimator performance. Fig. 6 depicts the estimator performance in term of MSE for QPSK data symbols, different mobile speeds and different spreading factor values L. The curves represent the MSE obtained with the analytical expression (12), and the markers those obtained by simulation. We note that the MSE measured by simulation are really close to those predicted with the MSE formula. This validates the analytical development made in the previous section. We note that beyond a given $\frac{E_b}{N_0}$, the MSE reaches a floor which is easily interpreted as being due to the MCI (12).

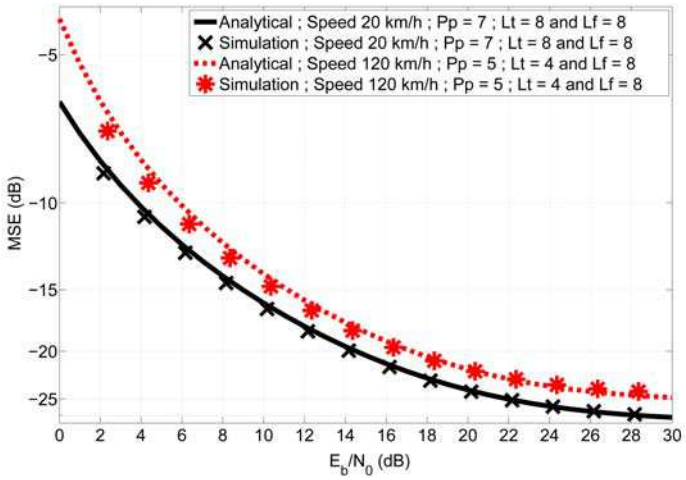

Fig. 6. MSE performance obtained with the analytical expression and by simulation - QPSK data symbols- Speeds: 20km/h and 120km/h - β= 0.003 and 0.018

Fig.7(a) and Fig.7(b) give the BER measured for 16QAM and 64QAM data symbols under the time-invariant channel models F1 and P1 respectively for both the DVB-T system and the proposed system. To quantify the loss due to CFR estimation error resulting from the MCI and the AWGN, we give the performance of the proposed system with perfect CFR estimation by subcarrier and perfect CFR estimation by subset of L subcarriers. According to (12), the BER degradation from perfect CFR estimation by subcarrier to perfect CFR estimation by subset of subcarriers is due to the MCI, and the degradation from perfect CFR estimation by subset of subcarriers to spread pilot CFR estimation is due to the AWGN. In

Fig. 7(a), the curves of the proposed system with perfect CFR estimation by subcarrier and those with perfect CFR estimation by subset of subcarriers overlap. Since the frequency spreading length is equal to 4, it means that the F1 channel model is very flat over four subcarriers. On the other hand, under P1 channel model, there is a degradation. This is explained by the P1 non-LOS characteristic which generates a higher selectivity in the frequency domain. Let us note for a BER equal to 10^{-4}, from perfect CFR estimation by subcarrier to spread pilot channel estimation, there is a loss of less than 1dB and 1.5dB under F1 and P1 channel models respectively. Since the F1 and P1 channel models do not vary in time, it is interesting to spread the symbols as much as possible in the time direction. For a time spreading length L_t larger or equal to 4 (which implies $L \geq 16 > 12$), a gain in term of spectral efficiency and useful bit rate is obtained compared to the DVB-T system. In most of the cases, for $L_t = 16$, the performance of the proposed system based on spread pilot CFR estimation slighly outperforms that of the DVB-T system with perfect CFR estimation.

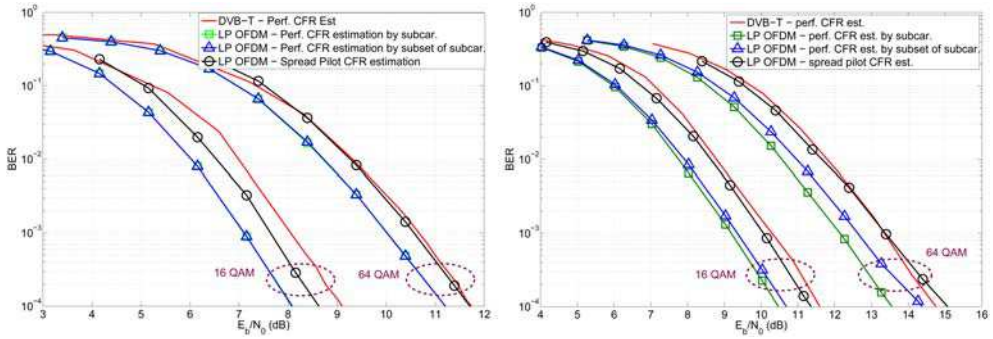

(a) F1 Channel (b) P1 Channel

Fig. 7. Performance comparison between the DVB-T system with perfect CFR estimation and the proposed 2D LP OFDM under time-invariant channel models - $R_c = \frac{1}{2}$ - $L_f = 4$ and $L_t = 16$ - $P_p = 7$

To verify if the MCI caused by the channel time variation does not degrade to much the proposed system performance, Fig.8 gives the BER measured under the TU6 channel model with a mobile speed of 20 km/h. In this case, since the channel varies both in frequency and time domains, it is necessary to optimize the time and frequency spreading lengths L_t and L_f for a given total spreading length. Fig. 8(a) gives the BER of the proposed system based on spread pilot CFR estimation for a given $\frac{E_b}{N_0}$ with a total spreading length equal to 64 for QPSK and 16QAM data symbols. The values of L_t and L_f giving the lowest BER are 16 and 4 respectively. Using these spreading length values, we compare the proposed system to the DVB-T system with perfect CFR estimation in Fig. 8(b). Likewise with time-invariant channels, the performances of the DVB-T system with perfect CFR estimation and the proposed system with spread pilot CFR estimation are similar. Furthermore, for a BER equal to 10^{-4}, the loss from perfect CFR estimation by subcarrier to spread pilot CFR estimation is further less than 1 dB. Since the time spreading length L_t is equal to 16, it proves that our proposed CFR estimation is not sensible to low mobility scenarios in term of BER. Obviously, for high velocities, degradations of the proposed system performance would be notable. To resolve this weakness, it is possible to extend the system to the space dimension

using a space code block code (SCBC). Indeed, it is established in [14] that a SCBC system based on spread pilot CFR estimation is very robust to high mobility scenarios.

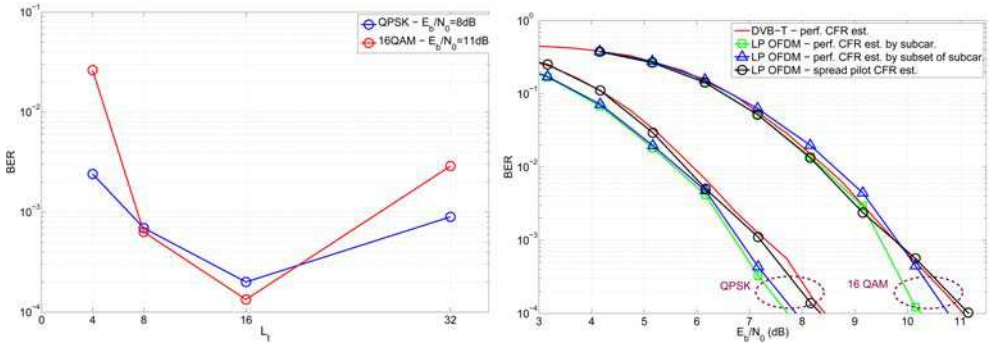

(a) L_t and L_f optimizations (b) BER performance - L_f = 4 and L_t = 16 - P_p = 7

Fig. 8. Performance comparison between the DVB-T system with perfect channel estimation and the proposed 2D LP OFDM under the TU6 mobile channel model - 20 km/h - β = 0.003 - L = 64

4. Synchronization principles

In the 2K mode (corresponding to a 2048 FFT size) of the DVB-T standard, 45 continual pilot subcarriers are reserved to help the receiver to estimate the CFO and the SFO. This additional pilot information once again reduces the spectral efficiency and the useful bit rate of the system. In our system based on spread pilots, we propose to exploit the pilot symbols already used for CFR estimation to estimate the CFO and the SFO. Thus, we avoid a new reduction in the spectral efficiency.

Two stages of CFO and SFO estimation are proposed. The first one dedicated to fine CFO estimation is processed before despreading the pilot symbols. The estimated CFO is then used to synchronize the received signal in the time domain. Nevertheless, as detailed hereafter, residual CFO will still be present after this initial synchronization step. The aim of the second synchronization stage is indeed to estimate and compensate for the residual CFO. To further exploit pilot information, it is possible during this stage to also estimate SFO, thus obtaining a joint residual CFO and SFO estimation.

In the following, we define the CFO ζ and the SFO ξ as:

$$\zeta = (F_{\mathrm{TX}} - F_{\mathrm{RX}})\, T_s \tag{13}$$

$$\xi = \frac{\Delta T}{T_s} \tag{14}$$

with F_{TX} and F_{RX} the carrier frequency of the transmitter and the receiver respectively, T_s the sampling period at the transmitter and ($T_s + \Delta T$) at the receiver.

A. Fine CFO estimation

Since each active subcarrier conveys a part of the spread pilot symbol information, a gain in diversity can be obtained compared to the DVB-T system which uses only a few pilot subcarriers for synchronization issues. Therefore, we propose to estimate the CFO before

despreading the pilot symbols. Neglecting the SFO effects which are much less significant than CFO [5], the received symbol in the presence of CFO during the qth OFDM symbol on the n'th subcarrier of the subset of subcarriers (t, s') corresponding to a component of vector $\mathbf{z}_{t,s'}$ in equation (3) expresses as follows:

$$\begin{aligned} z_{t,s'}[q,n'] &= \mathrm{e}^{j2\pi q(N+\upsilon)\zeta} \sum_{s=0}^{S-1} \sum_{n=0}^{L_f-1} y_{t,s}[q,n]\, h_{t,s}[q,n]\, \varphi(s',s,n',n) + w_{t,s'}[q,n'] \\ &= \mathrm{e}^{j2\pi q(N+\upsilon)\zeta}\, y_{t,s'}[q,n']\, h_{t,s'}[q,n']\, \varphi(s',s',n',n') + \Xi_{\mathrm{ICI}}(t,s',q,n') + w_{t,s'}[q,n'] \end{aligned} \tag{15}$$

where $\varphi(s',\ s,\ n',\ n)$ is an equivalent transfer function describing the attenuation and the phase rotation caused by the CFO. It is equal to:

$$\varphi(s',s,n',n) = \psi_N\left(\zeta + \frac{(s'-s)L_f + (n'-n)}{N}\right) \exp\left\{j\pi(N-1)\left(\zeta + \frac{(s'-s)L_f + (n'-n)}{N}\right)\right\} \tag{16}$$

where $\psi_N(x)$ is the Dirichlet function defined by: $\psi_N(x) = \frac{\sin(\pi N x)}{N\sin(\pi x)}$. The second term $\Xi_{\mathrm{ICI}}(t,s',q,n')$ in (15) is the ICI coming from the other active subcarriers in the same OFDM symbol. It writes:

$$\Xi_{\mathrm{ICI}}(t,s',q,n') = e^{j2\pi q(N+\upsilon)\zeta} \left(\underbrace{\sum_{\substack{n=0 \\ n\neq n'}}^{L_f-1} y_{t,s'}[q,n]\, h_{t,s'}[q,n]\, \varphi(s',s',n',n)}_{\text{ICI from the interested sub-band } s'} + \underbrace{\sum_{\substack{s=0 \\ s\neq s'}}^{S-1} \sum_{n=0}^{L_f-1} y_{t,s}[q,n]\, h_{t,s}[q,n]\, \varphi(s',s,n',n)}_{\text{ICI from the other sub-bands } s\neq s'} \right) \tag{17}$$

The phase rotation at the left-hand side of (15) is due to the CFO increment in time. It is clear that this phase rotation increases with the OFDM symbol index q. Thus, we will benefit from this increment to define the CFO estimation metric $\Gamma_t(\zeta)$ computed at the t-th frame from the pilot sequence by:

$$\begin{aligned} &\Gamma_t(\zeta) \\ &= \sum_{q=0}^{L_t-2} \sum_{s'=0}^{S-1} \sum_{n'=0}^{L_f-1} c_p[n'L_t+q]\, z^*_{t,s'}[q,n']\, c^*_p[n'L_t+q+1]\, z_{t,s'}[q+1,n'] \\ &= \sum_{q=0}^{L_t-2} \sum_{s'=0}^{S-1} \sum_{n'=0}^{L_f-1} c_p[n'L_t+q] \left\{ \mathrm{e}^{-j2\pi q(N+\upsilon)\zeta}\, y^*_{t,s'}[q,n']\, h^*_{t,s'}[q,n']\, \varphi^*(s',s',n',n') + \Xi^*_{\mathrm{ICI}}(t,s',q,n') + w^*_{t,s'}[q,n'] \right\} \\ &\times c^*_p[n'L_t+q+1] \left\{ \mathrm{e}^{j2\pi(q+1)(N+\upsilon)\zeta}\, y_{t,s'}[q+1,n']\, h_{t,s'}[q+1,n']\, \varphi(s',s',n',n') + \Xi_{\mathrm{ICI}}(t,s',q+1,n') + w_{t,s'}[q+1,n'] \right\} \end{aligned} \tag{18}$$

Assuming the channel does not vary over two consecutive OFDM symbols, i. e. $h_{t,s'}[(q,q+1),n'] = h_{t,s'}[q,n'] = h_{t,s'}[q+1,n']$ and using (2), the estimation metric finally writes:

$$\begin{aligned} \Gamma_t(\zeta) &= \frac{P_p}{L}\, e^{j2\pi(N+\nu)\zeta} \sum_{s'=0}^{S-1} |x_{t,s'}[p]|^2 \sum_{q=0}^{L_t-2} \sum_{n'=0}^{L_f-1} |h_{t,s'}[(q,q+1),n']|^2 + \Xi(t,s',q,n') \\ &= \frac{P_p}{L}\, S\, N_u\, (L_t-1)\, e^{j2\pi(N+\nu)\zeta} + \sum_{s'=0}^{S-1} \sum_{n'=0}^{L_f-1} \sum_{q=0}^{L_t-2} \Xi(t,s',q,n') \end{aligned} \tag{19}$$

where $\Xi(t,\ s',\ q,\ n')$ results from the contributions of the interferences caused by the data chips superimposed to the pilot chips, the ICI due to CFO and the AWGN. In our study, we assumed that these interferences have Gaussian distribution with zero mean [15] [16]. Consequently, if the product $S \times L_f \times (L_t - 1)$ is large enough:

$$\sum_{s'=0}^{S-1} \sum_{n'=0}^{L_f-1} \sum_{q=0}^{L_t-2} \Xi(t, s', q, n') \to 0 \tag{20}$$

Using (18) and (20), it is straightforward to say that the CFO is the measure of the phase of $\Gamma_t(\zeta)$:

$$\hat{\zeta}_t^{(\text{fine})} = \frac{1}{j2\pi(N+\nu)} \arg\{\Gamma_t(\zeta)\} \tag{21}$$

It should be noted that to avoid any phase ambiguity, it is necessary that:

$$|2\pi(N+\nu)\zeta| < \pi \tag{22}$$

This constraint determinates the maximum estimable CFO value at this stage. For instance, in the 2K mode, with a relative guard interval size equal of 1/4, the maximum estimable CFO is 40% of the intercarrier spacing $\frac{1}{NT_s}$. Let us remind that the widely used guard interval based coarse carrier frequency synchronization [17] [18] brings down the CFO to such values, which makes the proposed algorithm compatible with classical OFDM reception schemes.

As depicted in Fig. 9, the estimated CFO $\hat{\zeta}_t^{(\text{fine})}$ value is used to correct the signal in the time domain in order to mitigate the ICI. To evaluate the performance of the proposed fine CFO estimation, we give in Fig. 10 the residual CFO after this synchronization step in open loop (in the case when no CFO loop filter is used). In other words, we give the average error of the instantaneous estimated CFO $\hat{\zeta}_t^{(\text{fine})}$. According to BER simulations obtained for CFR estimation, the frequency spreading length Lf is set to 4. However, we reduce the time spreading length Lt to 8. The CFO value is set to 10% of the intercarrier spacing. It can be seen that the residual CFO falls down less than 2% whatever the SNR or the channel condition. On the other hand, we notice that under the TU6 channel model, the residual CFO values are very similar for any mobility scenario. From (18) and (19), we know that the phase rotation measurement used to estimate the CFO is carried out between two consecutive OFDM symbols under a constraint of flatness of the channel in the time domain over two OFDM symbols. This constraint is reasonable even in high mobility scenarios, which explains why the proposed fine CFO estimation method is not sensitive to velocity variations. Moreover, we remark that beyond a given $\frac{E_b}{N_0}$ value, residual CFO curves reach a plateau. Since the CFO estimation is processed before the deprecoding function, this error floor is due to the data chips interference. This motivates for the use of a second estimation step processed after deprecoding function.

B. Joint residual CFO and SFO estimation

In order to mitigate the data chips interference, we propose to add a second stage of CFO and SFO estimations after the deprecoding function. Thus, if the spreading lengths L_t and L_f

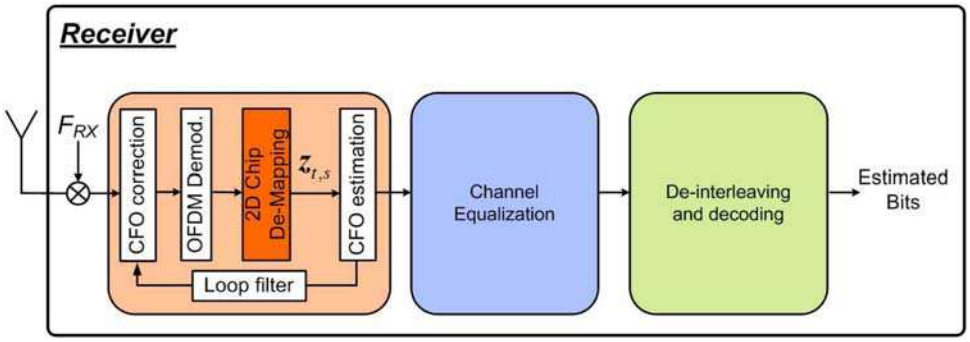

Fig. 9. Fine CFO estimation scheme before despreading function

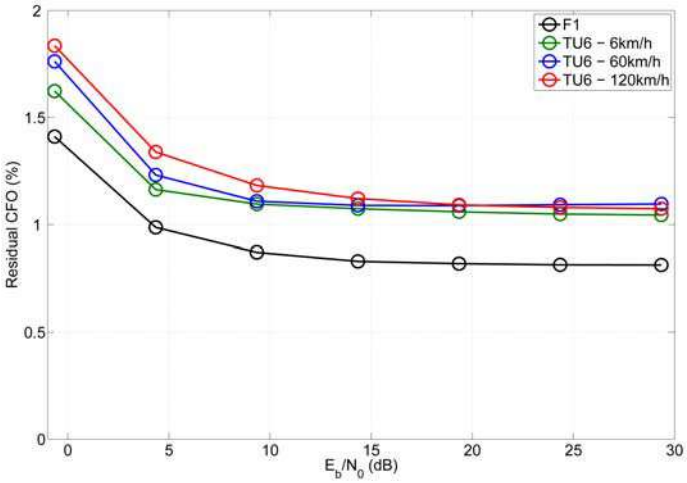

Fig. 10. Residual CFO after the 1st synchronization stage in open loop - SFO null - L_f = 4 and L_t = 8 - 16QAM data symbols

have been optimized such as the channel is flat enough over each subset of subcarriers, the interference from the data symbols should be strongly attenuated after the deprecoding function.

First of all, let us derive the expression of the received symbol on the n'th subcarrier during the qth OFDM symbol of the subset of subcarriers (t, s') after the first stage of synchronization, before the deprecoding function:

$$z_{t,s'}[q,n'] = \sum_{s=0}^{S-1}\sum_{n=0}^{L_f-1} \exp\left\{j2\pi q\left(N+\upsilon\right)\left(\zeta^{(\mathrm{res})}+\frac{sL_f+n}{N}\xi\right)\right\} y_{t,s}[q,n]\, h_{t,s}[q,n]\, \varphi(q,s',s,n',n) + w_{t,s'}[q,n'] \quad (23)$$

with $\varphi(q,s',s,n',n) = \psi_N\left(\zeta^{(\mathrm{res})}+\frac{sL_f+n}{N}\xi+\frac{(s'-s)L_f+(n'-n)}{N}\right)\exp\left\{j\pi\left(N-1\right)\left(\zeta^{(\mathrm{res})}+\frac{sL_f+n}{N}\xi+\frac{(s'-s)L_f+(n'-n)}{N}\right)\right\}$. To simplify equation (23), we define $\phi_{t,s'}[q,n']$

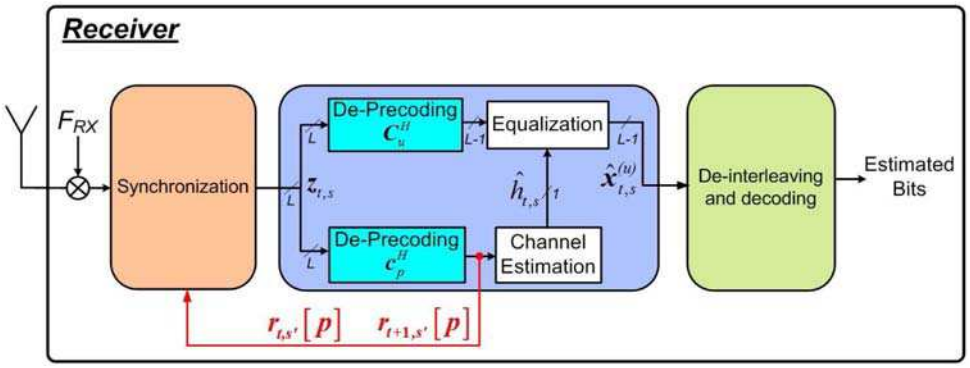

Fig. 11. Joint residual CFO and SFO estimation scheme after the deprecoding function

as the function describing the total phase rotation and $\psi_{t,s'}[q,n']$ as the function describing the amplitude attenuation caused by CFO and SFO on the interested subcarrier.

$$\phi_{t,s'}[q,n'] = \exp\left\{j2\pi q\left(N+\nu\right)\left(\zeta^{(\text{res})}+\frac{sL_f+n}{N}\xi\right)\right\}\exp\left\{j\pi\left(N-1\right)\left(\zeta^{(\text{res})}+\frac{sL_f+n}{N}\xi\right)\right\} \quad (24)$$

$$\psi_{t,s'}[q,n'] = \psi_N\left(\zeta^{(\text{res})}+\frac{sL_f+n}{N}\xi\right) \quad (25)$$

Hence, the expression of the received symbol on the interested subcarrier (23) can be simplified and re-expressed as:

$$z_{t,s'}[q,n'] = y_{t,s'}[q,n']\,h_{t,s'}[q,n']\,\phi_{t,s'}[q,n']\,\psi_{t,s'}[q,n'] + \Xi_{\text{ICI}}(t,s',q,n') + w_{t,s'}[q,n'] \quad (26)$$

Now, let us develop the expression of the received pilot symbol on the subset of subcarriers (t, s') after deprecoding by pilot sequence $\mathbf{c}_p^{\text{H}}$:

$$r_{t,s'}[p] = \mathbf{c}_p^H\left[\Phi_{t,s'}\,\Psi_{t,s'}\,\mathbf{H}_{t,s'}\,\mathbf{C}\,\mathbf{P}\,\mathbf{x}_{t,s'} + \Xi_{\text{ICI}}(t,s') + \mathbf{w}_{t,s'}\right] \quad (27)$$

where $\Phi_{t,s'} = \text{diag}\{\phi_{t,s'}[0,0]\ldots\phi_{t,s'}[q,n']\ldots\phi_{t,s'}[L_t-1,L_f-1]\}$ and $\Psi_{t,s'} = \text{diag}\{\psi_{t,s'}[0,0]\ldots\psi_{t,s'}[q,n']\ldots\psi_{t,s'}[L_t-1,L_f-1]\}$ are the $[L \times L]$ diagonal matrices which components are the phase rotations and the attenuation factors respectively, due to CFO and SFO on the L received symbols over the subset of subcarriers (t, s'). To simplify equation (27), we define the equivalent channel matrix as $\mathbf{H}_{t,s'}^{(\text{eq})} = \Phi_{t,s'}\,\Psi_{t,s'}\,\mathbf{H}_{t,s'}$. Hence, the received pilot symbol can be rewritten as:

$$r_{t,s'}[p] = \mathbf{c}_p^H\left[\mathbf{H}_{t,s'}^{(\text{eq})}\,\mathbf{C}\,\mathbf{P}\,\mathbf{x}_{t,s'} + \Xi_{\text{ICI}}(t,s') + \mathbf{w}_{t,s'}\right] \quad (28)$$

Finally, using (4) and (5), the received pilot symbol over the subset of subcarriers (t, s') writes:

$$\begin{aligned} r_{t,s'}[p] &= \overline{h}_{t,s'}^{(\text{eq})}\sqrt{P_p}\,x_{t,s'}[p] + \Xi'_{\text{ICI}}(t,s') + \Xi_{\text{MCI}}(t,s') + \Xi_{\text{WGN}}(t,s') \\ &= \overline{\phi}_{t,s'}\,\overline{\psi}_{t,s'}\,\overline{h}_{t,s'}\,\sqrt{P_p}\,x_{t,s'}[p] + \Xi(t,s') \end{aligned} \quad (29)$$

where $\overline{\phi}_{t,s'}$ and $\overline{\psi}_{t,s'}$ are the average phase rotation and the average attenuation factor due to CFO and SFO over the subset of subcarriers (t, s').

To jointly estimate the residual CFO and the SFO, we propose to measure the phase rotation between two consecutive frames t and (t + 1). First of all, let us derive the expressions of the phase rotations $\overline{\phi}_{t,s'}$ and $\overline{\phi}_{t+1,s'}$ which are the average phase rotations associated to sub-band s' during frames t and (t + 1) respectively:

$$\begin{aligned}\overline{\phi}_{t,s'} &= \frac{1}{L}\sum_{q=0}^{L_t-1}\sum_{n'=0}^{L_f-1}\phi_{t,s'}[q,n'] \\ &= \pi(N-1)\left[\zeta^{(\text{res})}+\frac{(2s'+1)L_f-1}{2N}\xi\right]+\pi(L_t-1)(N+\nu)\left[\zeta^{(\text{res})}+\frac{(s'+1)L_f-1}{N}\xi\right]\end{aligned} \tag{30}$$

$$\overline{\phi}_{t+1,s'} = \overline{\phi}_{t,s'} + 2\pi L_t(N+\nu)\left[\zeta^{(\text{res})}+\frac{(2s'+1)L_f-1}{2N}\xi\right] \tag{31}$$

By neglecting the interference term $\Xi(t,\ s')$, we define the CFO/SFO estimation metric on sub-band s':

$$\begin{aligned}\Theta_{(t,t+1),s'} &= \arg\left\{\left(\frac{r_{t+1,s'}[p]}{x_{t+1,s'}[p]}\right)\left(\frac{r_{t,s'}[p]}{x_{t,s'}[p]}\right)^*\right\} \\ &= \left(\overline{\phi}_{t+1,s'}+\arg\left\{\overline{h}_{t+1,s'}\right\}\right)-\left(\overline{\phi}_{t,s'}+\arg\left\{\overline{h}_{t,s'}\right\}\right)\end{aligned} \tag{32}$$

Assuming that $\overline{h}_{t,s'}=\overline{h}_{t+1,s'}$, i.e. the channel does not vary during (2 × L_t) OFDM symbols, the effect of the CFR disappears and (32) becomes:

$$\begin{aligned}\Theta_{(t,t+1),s'} &= \overline{\phi}_{t+1,s'}-\overline{\phi}_{t,s'} \\ &= 2\pi L_t(N+\nu)\left[\zeta+\frac{(2s'+1)L_f-1}{2N}\xi\right] \\ &= 2\pi L_t(N+\nu)\left[\zeta+\frac{L_f-1}{2N}\xi+\frac{L_f}{N}\xi s'\right]\end{aligned} \tag{33}$$

Hence, using a least square estimator it is possible to estimate both the residual CFO and the SFO:

$$\hat{\xi}=\frac{\sum_{s'=0}^{S-1}(s'-\overline{s}')\left(\Theta'_{(t,t+1),s'}-\overline{\Theta}'_{(t,t+1)}\right)}{\sum_{s'=0}^{S-1}(s'-\overline{s}')^2}\times\frac{N}{L_f} \tag{34}$$

$$\hat{\zeta}^{(\text{res})}=\overline{\Theta}'_{(t,t+1)}-\frac{L_f-1}{2N}\hat{\xi} \tag{35}$$

where $\Theta'_{(t,t+1),s'}=\Theta_{(t,t+1),s'}/(2\pi L_t(N+\nu))$, $\overline{\Theta}'_{(t,t+1)}=\frac{1}{S}\sum_{s'=0}^{S-1}\Theta'_{(t,t+1),s'}$ and $\overline{s}'=\frac{1}{S}\sum_{s'=0}^{S-1}s'$. Similarly to the previous CFO estimation stage, we notice that to avoid any phase ambiguity, it is necessary that:

$$2\pi L_t(N+\nu)\left[\zeta+\frac{L_f-1}{2N}\xi+\frac{L_f}{N}\xi s'\right]<\pi \tag{36}$$

Using the simulation parameters given in Table I, if the SFO is null, (36) implies a maximum estimable residual CFO value equal to 2.5% and 5% of the intersubcarrier spacing, for a time spreading length equal to 8 and 16 respectively. Since the maximum residual CFO at the output of the initial synchronization stage is lower than 2%, the proposed residual CFO estimation is well suitable.

To analyse the performance of the joint residual CFO and SFO estimation after deprecoding function, we give in Fig. 12 the final residual CFO and SFO measured at the output of the 2nd synchronization stage, in open loop, using the simulation parameters given in Table II. We set the CFO value to 2% of the intersubcarrier spacing which is the largest value resulting from the initial synchronization step. To highlight the influence of the time spreading length L_t and the mobile velocity on the estimators, the simulations have been carried out for two different L_t values and different mobility scenarios under the TU6 channel model. As expected, the proposed residual CFO estimation after deprecoding function allows the CFO to be advantageously reduced compared to the values obtained with the fine CFO estimation before deprecoding function. Indeed, for any mobility scenario and any $\frac{E_b}{N_0}$ value, the final residual CFO measured at the output of the 2nd synchronization stage is lower than 0.55% whereas it is higher than 1% after the initial synchronization step. Similarly to the residual CFO at the output of the initial synchronization stage, beyond a given $\frac{E_b}{N_0}$ value, the final residual CFO and SFO curves reach a floor due to the MCI. It appears that for moderate mobility scenarios (until 60km/h), the final residual CFO and SFO are similar for a time spreading length L_t both equal to 4 and 8. On the other hand, for high mobility scenarios, the higher the L_t value, the more significant the final residual CFO and SFO. It is explained by the fact that the constraint of flatness of the channel is all the more drastic than the L_t value gets higher, which translates into a higher sensitivity of our algorithm in high mobility scenarios.

Fig. 13 gives the global system performance in term of BER under the TU6 channel model. The CFO and SFO values are set to 10% and 100ppm respectively. The BER curves for QPSK and 16QAM data symbols have been simulated for a mobile velocity equal to 120km/h and 60km/h respectively. The DVB-T system performance is given as reference with perfect CFR estimation and perfect synchronization. To focus on the intrinsec performance of the proposed frequency synchronization method, perfect CFR estimation by subcarrier is

Bandwidth	8 MHz
FFT size N_{FFT}	2048 samples
Guard Interval size	512 samples (64 μs)
OFDM symbol duration T_{OFDM}	280 μs
Carrier frequency	500 MHz
Data symbol constellations	QPSK - 16QAM
Pilot symbol constellation	BPSK
Convolutional code rate	$R_c = 1/2$ using $(133, 171)_o$
Frequency spreading length	$L_f = 4$
Channel model	TU6
Mobile Speeds	20km/h - 60km/h - 120km/h
Relative Doppler Frequencies β	0.003 - 0.014 - 0.028
Relative Carrier Frequency Offset	10%
Relative Residual Carrier Frequency Offset $\zeta^{(\text{res})}$	2%
Relative Sampling Frequency Offset ξ	100 ppm
Loop filter gain for CFO estimation	1/16
Loop filter gain for SFO estimation	1/64

Table II Simulation parameters

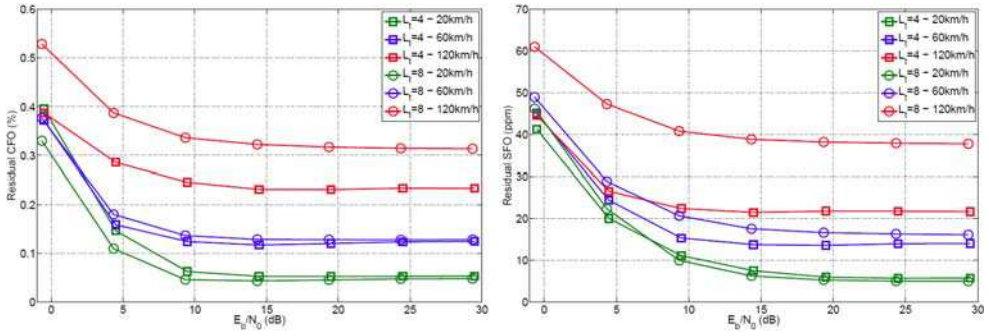

(a) Residual CFO - $\zeta^{(res)} = 2\%$ and $\xi = 0$ (b) Residual SFO - $\zeta^{(res)} = 0$ and $\xi = 100$ppm

Fig. 12. Residual CFO and SFO after the 2nd synchronization stage - 16QAM data symbols - TU6 channel - $L_f = 4$

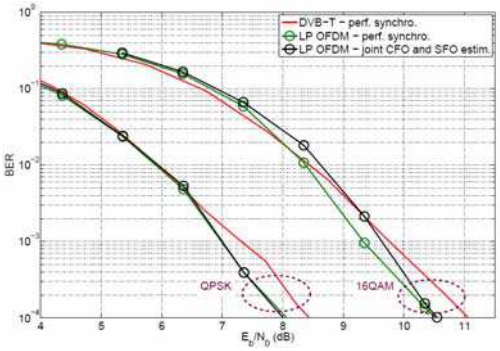

Fig. 13. BER performance under TU6 channel - Mobile Speed: 120km/h for QPSK and 60km/h for 16QAM - $R_c = 1/2$ - $\zeta = 1\%$ and $\xi = 100$ppm - $L_f = 4$ and $L_t = 8$

assumed. The final estimated CFO and SFO values used to synchronize the received signal are those obtained at the output of the loop filters which gains values are set as in [5]. Similarly to CFR estimation simulations, the proposed system based on spread pilot synchronization slightly outperforms the DVB-T system with perfect synchronization. Moreover, the performance of the proposed synchronization method is very close to perfect synchronization case. It proves that the impact of such residual CFO and SFO values on BER performance are negligeable and thus validates the benefit of the proposed CFO and SFO estimation techniques.

5. Conclusion

In this study, we proposed an efficient and very simple joint CFR, CFO and SFO estimation based on spread pilots for digital video broadcasting systems. The specificity in the LP OFDM waveform based on spread pilots is that all the active subcarriers convey a part of the pilot information, contrary to the classical OFDM systems in which only a few subcarriers are defined as pilot. It allows to not have to define different pilot symbols for each estimation algorithms. Thus, it avoids a reduction of the spectral efficiency and the useful bit rate of the system.

In contrast to classical existing OFDM systems, a deprecoding function is used instead of an interpolating filtering technique for CFR estimation. Therefore, the CFR estimation is highly simplified. Nevertheless, an interference term from data symbols appears in the estimators. This interference term called MCI is function of the autocorellation of the channel for the estimations carried out after despreading the pilot symbols. To avoid a significant degradation of the system performance, the time and frequency spreading lengths can be optimized depending on the channel characteristics. Let us note that an interference cancellation based on data decision directed could mitigate the MCI.
Two synchronization stages have been proposed. The first one processed before deprecoding function is dedicated to fine CFO estimation which brings down the CFO to less than 2% of the intersubcarrier spacing in open loop for any mobility scenario. The second one is applied after despreading the pilots symbols. It estimates both the residual CFO and the SFO. Although, it is more sensitive to high mobility scenarios, it improves the CFO estimation and diminuates the final residual CFO to a value lower than 0.55% in open loop. Finally, the simulations show that the proposed synchronization algorithm performance in term of BER is very close to perfect synchronization case in closed loop.
To conclude, the proposed system based on spread pilots is more flexible due to the possible adaptation of the time and frequency spreading lengths. It offers an improvement of the spectral efficiency and the useful bit rate which is stated in Table III. Eventually, taking into account the power loss due to pilot symbol insertion, it slightly outperforms the DVB-T system with perfect CFR estimation and perfect frequency synchronization.

Bandwidth	8 MHz
FFT size N_{FFT}	2048 samples
Guard Interval size	512 samples (64 μs)
OFDM symbol duration T_{OFDM}	280 μs
Convolutional code rate	$R_c = 1/2$ using $(133, 171)_o$
Useful bit rates of DVB-T system	4.98 Mbits/s for QPSK 9.95 Mbits/s for 16QAM 14.93 Mbits/s for 64QAM
Useful bit rates of 2D LP OFDM for QPSK	5.33 Mbits/s for $L = 16$ 5.51 Mbits/s for $L = 32$ 5.60 Mbits/s for $L = 64$
Useful bit rates of 2D LP OFDM for 16QAM	10.66 Mbits/s for $L = 16$ 11.02 Mbits/s for $L = 32$ 11.20 Mbits/s for $L = 64$
Useful bit rates of 2D LP OFDM for 64QAM	15.99 Mbits/s for $L = 16$ 16.53 Mbits/s for $L = 32$ 16.80 Mbits/s for $L = 64$

Table III Useful bit rates of the DVB-T system of 2D LP OFDM system

6. Acknowledgement

This work was supported by the French national project “Mobile TV World” and the European project CELTIC B21C (“Broadcast for 21st Century”) [19].

Appendix

In this section, a property from the random matrix and free probability theories is defined for the computation of the MCI variance (7). Furthermore, the computation of the autocorrelation function of the channel R_{HH} is carried out.

Random matrix and free probability theories property

Let **C** be a Haar distributed unitary matrix [13] of size [$L \times L$]. $\mathbf{C} = (\mathbf{c}_p, \mathbf{C}_u)$ can be decomposed into a vector $\mathbf{c}_p$ of size [$L \times 1$] and a matrix $\mathbf{C}_u$ of size [$L \times (L-1)$]. Given these assumptions, it is proven in [20] that:

$$\mathbf{C}_u \, \mathbf{P}'_u \, \mathbf{C}_u^{\mathrm{H}} \xrightarrow{L \to \infty} \alpha P_u \left(I - \mathbf{c}_p \, \mathbf{c}_p^{\mathrm{H}} \right) \tag{37}$$

where $\alpha = 1$ is the system load and $P_u = 1$ is the power of the interfering users.

Autocorrelation function of the channel

The autocorrelation function of the channel writes:

$$R_{HH}(\Delta q, \Delta n) = E\left\{ H_{t,s}[q,n] \, H^*_{t,s}[q - \Delta q, n - \Delta n] \right\} \tag{38}$$

We can express the frequency channel coefficients $H_{t,s}[q, n]$ as a function of the channel impulse response (CIR):

$$H_{t,s}[q,n] = \sum_{k=0}^{N_{\mathrm{FFT}}-1} \gamma_{t,q}[k] \, e^{-2j\pi \frac{\left(sL_f + n\right)}{N_{\mathrm{FFT}}} k} \tag{39}$$

where $\gamma_{t,q}[k]$ is the complex amplitude of the kth sample of the CIR during the qth OFDM symbol of the mth frame, and N_{FFT} is the FFT size. Therefore, by injecting (39) in (38), the autocorrelation function of the channel can be rewritten as:

$$R_{HH}(\Delta q, \Delta n) = \frac{1}{N_{\mathrm{FFT}}} \sum_{k=0}^{N_{\mathrm{FFT}}-1} \sum_{k'=0}^{N_{\mathrm{FFT}}-1} \mathrm{E}\left\{ \gamma_{t,q}[k] \, \gamma^*_{t,q-\Delta q}[k'] \right\} e^{-2j\pi \frac{\Delta n}{N_{\mathrm{FFT}}} k} \tag{40}$$

Since different taps of the CIR are uncorrelated, it comes:

$$R_{HH}(\Delta q, \Delta n) = \frac{1}{N_{\mathrm{FFT}}} \sum_{k=0}^{N_{\mathrm{FFT}}-1} \mathrm{E}\left\{ \gamma_{t,q}[k] \, \gamma^*_{t,q-\Delta q}[k] \right\} e^{-2j\pi \frac{\Delta n}{N_{\mathrm{FFT}}} k} \tag{41}$$

According to Jake's model [21], the correlation of the kth sample of the CIR is:

$$\mathrm{E}\left\{ \gamma_{t,q}[k] \, \gamma^*_{t,q-\Delta q}[k] \right\} = \rho_k J_0 \left(2\pi f_D \Delta q T_{\mathrm{OFDM}} \right) \tag{42}$$

where ρ_k is the power of the kth sample of the CIR, $J_0(.)$ the zeroth-order Bessel function of the first kind, f_D the maximum Doppler frequency and T_{OFDM} the total OFDM symbol duration. Finally, the autocorrelation function of the channel (41) can be expressed as:

$$R_{HH}(\Delta q, \Delta n) = \frac{1}{N_{\mathrm{FFT}}} \sum_{k=0}^{N_{\mathrm{FFT}}-1} \rho_k e^{-2j\pi \frac{\Delta n}{N_{\mathrm{FFT}}} k} J_0 \left(2\pi f_D \Delta q T_{\mathrm{OFDM}} \right) \tag{43}$$

7. References

[1] S. Weinstein and P. Ebert, "Data Transmission by Frequency-Division Multiplexing Using the Discrete Fourier Transform," *IEEE Trans. Commun.*, vol. 19, no. 5, pp. 628–634, Oct. 1971.

[2] ETSI EN 300 744, "Digital Video Broadcasting (DVB) ; Framing structure channel coding and modulation for digital terrestrial television," Tech. Rep., Nov. 2004.

[3] P. Höfer, S. Kaiser, and P. Robertson, "Two-dimensional pilot-symbol-aided channel estimation by Wiener filtering," *ICASSP-97*, vol. 3, pp. 184–1848, 1997.
[4] H. Steendam and M. Moeneclaey, "Sensitivity of orthogonal frequency-division multiplexed systems to carrier and clock synchronization errors," *Signal Processing*, vol. 80, pp. 1217–1229, 2000.
[5] S. A. Fechtel, "OFDM carrier and sampling frequency synchronization and its performance on stationary and mobile channels," *IEEE Trans. Consum. Electron.*, vol. 46, pp. 438–441, Aug. 2000.
[6] O. P. Pasquero, M. Crussière, Y. Nasser, and J.-F. Hélard, "2D Linear Precoded OFDM for Future Mobile Digital Video Broadcasting," *Signal Processing Advances in Wireless Communications, 2008 IEEE 9th Workshop on*, 2008.
[7] P. Shlichta, "Higher-dimensional hadamard matrices," *Information Theory, IEEE Transactions on*, vol. 25, no. 5, pp. 566–572, Sep 1979.
[8] N. Kuroyanagi and L. Guo, "Proposal of an alternate m-sequence spread spectrum system," vol. 1, Oct 1993, pp. 41–46 vol.1.
[9] N. Chapalain, D. Mottier, and D. Castelain, "Performance of uplink ss-mc-ma systems with frequency hopping and channel estimation based on spread pilots," *Personal, Indoor and Mobile Radio Communications, 2005. PIMRC 2005. IEEE 16th International Symposium on*, vol. 3, pp. 1515–1519 Vol. 3, Sept. 2005.
[10] C. Ho, B. Farhang-Boroujeny, and F. Chin, "Added pilot semi-blind channel estimation scheme for ofdm in fading channels," *Global Telecommunications Conference, 2001. GLOBECOM '01. IEEE*, vol. 5, pp. 3075–3079 vol.5, 2001.
[11] B. Molnar, I. Frigyes, Z. Bodnar, and Z. Herczku, "The wssus channel model: comments and a generalisation," *Global Telecommunications Conference, 1996. GLOBECOM '96. 'Communications: The Key to Global Prosperity*, pp. 158–162, Nov 1996.
[12] J. Evans and D. Tse, "Large system performance of linear multiuser receivers in multipath fading channels," *Information Theory, IEEE Transactions on*, vol. 46, no. 6, pp. 2059–2078, Sep 2000.
[13] M. Debbah, W. Hachem, P. Loubaton, and M. de Courville, "Mmse analysis of certain large isometric random precoded systems," *Information Theory, IEEE Transactions on*, vol. 49, no. 5, pp. 1293–1311, May 2003.
[14] O. P. Pasquero, M. Crussière, Y. Nasser, and J.-F. Hélard, "Efficient space code block code mimo channel estimation for future mobile video broadcasting," *Wireless Communications and Networking Conference, 2009. WCNC 2009. IEEE*, pp. 1–6, April 2009.
[15] T. Pollet, M. Van Bladel, and M. Moeneclaey, "BER Sensitivity of OFDM Systems to Carrier Frequency Offset and Wiener Phase Noise," *IEEE Trans. Commun.*, vol. 43, pp. 191–193, Feb/Mar/Apr 1995.
[16] Y. Nasser, M. Noes, L. Ros, and G. Jourdain, "Sensitivity of OFDM-CDMA Systems to Carrier Frequency Offset," *Communications, ICC 2006. IEEE International Conference on*, vol. 10, pp. 4577–4582, June 2006.
[17] H. Zhou, A. Malipatil, and Y.-F. Huang, "Synchronization issues in ofdm systems," Dec. 2006, pp. 988–991.
[18] M. Speth, S. Fechtel, G. Fock, and H. Meyr, "Optimum receiver design for ofdm-based broadband transmission .ii. a case study," *Communications, IEEE Transactions on*, vol. 49, no. 4, pp. 571–578, Apr 2001.
[19] http://www.celtic initiative.org/Projects/B21C.
[20] J.-M. Chaufray, W. Hachem, and P. Loubaton, "Asymptotic analysis of optimum and suboptimum cdma downlink mmse receivers," *Information Theory, IEEE Transactions on*, vol. 50, no. 11, pp. 2620–2638, Nov. 2004.
[21] W. Jakes, Ed., *Microwave Mobile Communications*. IEEE Press, 1994.

Digital Video

Edited by Floriano De Rango

ISBN 978-953-7619-70-1
Hard cover, 500 pages
Publisher InTech
Published online 01, February, 2010
Published in print edition February, 2010

This book tries to address different aspects and issues related to video and multimedia distribution over the heterogeneous environment considering broadband satellite networks and general wireless systems where wireless communications and conditions can pose serious problems to the efficient and reliable delivery of content. Specific chapters of the book relate to different research topics covering the architectural aspects of the most famous DVB standard (DVB-T, DVB-S/S2, DVB-H etc.), the protocol aspects and the transmission techniques making use of MIMO, hierarchical modulation and lossy compression. In addition, research issues related to the application layer and to the content semantic, organization and research on the web have also been addressed in order to give a complete view of the problems. The network technologies used in the book are mainly broadband wireless and satellite networks. The book can be read by intermediate students, researchers, engineers or people with some knowledge or specialization in network topics.

How to reference

In order to correctly reference this scholarly work, feel free to copy and paste the following:

Oudomsack Pierre Pasquero, Matthieu Crussière, Youssef Nasser, Eddy Cholet and Jean-François Hélard (2010). A New Waveform based on Linear Precoded Multicarrier Modulation for Future Digital Video Broadcasting Systems, Digital Video, Floriano De Rango (Ed.), ISBN: 978-953-7619-70-1, InTech, Available from: http://www.intechopen.com/books/digital-video/a-new-waveform-based-on-linear-precoded-multicarrier-modulation-for-future-digital-video-broadcastin

INTECH
open science | open minds

InTech Europe
University Campus STeP Ri
Slavka Krautzeka 83/A
51000 Rijeka, Croatia
Phone: +385 (51) 770 447
Fax: +385 (51) 686 166
www.intechopen.com

InTech China
Unit 405, Office Block, Hotel Equatorial Shanghai
No.65, Yan An Road (West), Shanghai, 200040, China
中国上海市延安西路65号上海国际贵都大饭店办公楼405单元
Phone: +86-21-62489820
Fax: +86-21-62489821